HHS Public Access

Author manuscript

Biomaterials. Author manuscript; available in PMC 2018 January 01.

Published in final edited form as:

Biomaterials. 2017 January ; 113: 80–92. doi:10.1016/j.biomaterials.2016.09.028.

An Immobilized Liquid Interface Prevents Device Associated Bacterial Infection In Vivo

Jiaxuan Chen[1,2], **Caitlin Howell**[2,3], **Carolyn A. Haller**[1,2], **Madhukar S. Patel**[1,2,4], **Perla Ayala**[1,2], **Katherine A. Moravec**[1], **Erbin Dai**[1], **Liying Liu**[1], **Irini Sotiri**[2,3], **Michael Aizenberg**[2], **Joanna Aizenberg**[2,3,5,*], and **Elliot L. Chaikof**[1,2,*]

[1]Beth Israel Deaconess Medical Center, Harvard Medical School, 330 Brookline Avenue, Boston, MA 02215.

[2]Wyss Institute of Biologically Inspired Engineering, Harvard University, 3 Blackfan Circle, Boston, MA 02115.

[3]John A. Paulson School of Engineering and Applied Sciences, Harvard University, 29 Oxford Street, Cambridge, MA 02138.

[4]Massachusetts General Hospital, Harvard Medical School, 55 Fruit Street, Boston, MA 02114.

[5]Department of Chemistry and Chemical Biology and Kavli Institute for Bionano Science and Technology, Harvard University, 12 Oxford Street, Cambridge, MA 02138.

Abstract

Virtually all biomaterials are susceptible to biofilm formation and, as a consequence, device-associated infection. The concept of an immobilized liquid surface, termed *slippery liquid-infused porous surfaces* (SLIPS), represents a new framework for creating a stable, dynamic, omniphobic surface that displays ultralow adhesion and limits bacterial biofilm formation. A widely used biomaterial in clinical care, expanded polytetrafluoroethylene (ePTFE), infused with various perfluorocarbon liquids generated SLIPS surfaces that exhibited a 99% reduction in *S. aureus* adhesion with preservation of macrophage viability, phagocytosis, and bactericidal function. Notably, SLIPS modification of ePTFE prevents device infection after *S. aureus* challenge in vivo, while eliciting a significantly attenuated innate immune response. SLIPS-modified implants also decrease macrophage inflammatory cytokine expression in vitro, which likely contributed to the presence of a thinner fibrous capsule in the absence of bacterial challenge. SLIPS is an easily

* Address correspondence to: Elliot L. Chaikof, M.D., Ph.D., Department of Surgery, Beth Israel Deaconess Medical Center, 110 Francis St, Suite 9F, Boston, MA 02115, Tel: (617) 632-9581, echaikof@bidmc.harvard.edu or Joanna Aizenberg, Ph.D., School of Engineering and Applied Sciences, Harvard University, 9 Oxford St, Pierce 229, Cambridge, MA 02138, Tel: (617) 495-3558, jaiz@seas.harvard.edu.

Author contributions: J.C., C.H. and C.A.H. designed research; J.C., C.H., P.A., K.A.M., E.D., L.L. and I.S. performed research; J.C., C.H., C.A.H., M.S.P., J.A., M.A. and E.L.C. analyzed data; and J.C., C.H., C.A.H., M.S.P., J.A., M.A. and E.L.C. wrote the paper.

Competing financial interests

J.A. is a founder of SLIPS Technologies, Inc. The other authors declare no competing financial interests.

implementable technology that provides a promising approach to substantially reduce the risk of device infection and associated patient morbidity, as well as health care costs.

Keywords

SLIPS; perfluorocarbon liquids; polytetrafluoroethylene; implant; infection; in vivo

1. Introduction

Device-associated infection is a major source of increased morbidity, mortality, and health care costs. In 2011, 4% of patients in U.S. acute care hospitals had at least one healthcare-associated infection, with one out of every four of these patients experiencing a device-associated infection [1]. The development of implant-associated infection can be attributed to the propensity of bacteria to form biofilms [2-5]. Distinct from bacteria in the free floating planktonic state, those growing in biofilms have diverse genotypes and phenotypes resulting in physiologic heterogeneity [6], which may lead to increased antimicrobial resistance [7, 8] and compromised host immune response [9, 10]. Further, the species dependent physical properties of biofilms, including extracellular matrix composition and roughness may limit penetration of conventional antimicrobials [11]. *Staphylococcus,* including *S. aureus* and *S. epidermidis,* are the most commonly isolated biomaterial colonizers and are typically responsible for infections of permanent implants [12].

Despite the wide variety of antifouling and antibacterial surface modifications, an ideal solution for the prevention of implant-associated infection does not exist. Current approaches can be broadly categorized into chemical or structural modifications, each with its own set of limitations. Chemical approaches have included the design of zwitterionic, mixed-charge, or amphiphilic thin films [13, 14], low-surface-energy materials [15, 16], and hydrophilic coatings, such as polyethylene glycol [17-19]; all of which have been designed to prevent nonspecific protein or cell adhesion. Hydrophilic ultrathin films of polyethylene glycol, as well as amphiphilic and charged films have displayed limited long-term stability in vivo and any defect in surface chemistry may serve as a nucleation site for bacterial attachment [20]. Likewise, substrates have been formulated to release compounds toxic to bacteria, such as antibiotics, quaternary ammonium salts, and silver ions [20, 21] or otherwise modified with tethered biocidal compounds, such as antimicrobial peptoid oligomers [22]. While these strategies have shown promise over short time periods, coatings designed to deliver bactericidal agents such as antibiotics, antiseptics, and nitrogen oxide have finite reservoirs and typically only last at therapeutic concentrations for days [21]. Moreover, both antibiotic- and silver-resistant pathogenic bacterial strains have emerged [23, 24]. Structural approaches have encompassed the design of micro- or nanoscale superhydrophobic surfaces to limit bacterial contact [25-27]. However, both micro- and nanoscale structures are susceptible to damage, as well as liquid infiltration. Furthermore, even if the chemical or physical modification persists and resists direct bacterial attachment, a bacteria or host generated conditioning layer of biomolecules and minerals often accumulates, which facilitates the formation of a biofilm atop this secondary film [20, 28].

The concept of an immobilized liquid interface has been recently introduced as a new strategy to create a stable dynamic surface that repels immiscible fluids, displays ultralow adhesion to both nano- and microscale solids, and is inherently self-healing [29, 30]. The design framework for such systems, termed a *slippery, liquid-infused, porous surface* (SLIPS), was inspired by the *Nepenthes* pitcher plant, which uses a layer of liquid water to create a low friction surface to prevent the attachment of insects [31]. The two primary features that are required to create an immobilized liquid surface include the capacity for physical entrapment of a liquid within a porous or nanostructured solid substrate and high chemical affinity between the liquid and solid as defined by surface energy parameters [29]. To date, the performance of SLIPS modified substrates have been largely studied in non-medical applications such as the creation of ice and frost repellent industrial materials[32], anti-fouling wearable fabrics[33], or as a means to limit biological fouling using in vitro [30, 34] or short-term ex vivo test systems [35]. In this report, we demonstrate the effectiveness of SLIPS-modified biomedical implants to resist device-associated infection after bacterial challenge in vivo. Expanded polytetrafluoroethylene (ePTFE) was selected as a model material given its prevalent use in clinical care in the form of prosthetic hernia meshes [36-38], grafts for cardiovascular reconstruction [39, 40], and as alloplastic implants in cosmetic and reconstructive surgery [41-43], as well as its known susceptibility to infection [44, 45]. As a porous, fluorinated implant material, ePTFE is readily amenable to infusion with fluorinated lubricants, such as perfluoropolyether (PFPE), perfluoroperhydrophenanthrene (PFPH), and perfluorodecalin (PFD). Of note, PFPH has demonstrated an acceptable safety profile in human studies as an intraoperative and postoperative tool in management of retinal tears [46]. Further, PFD has been evaluated in preclinical studies as a blood substitute [47] and is currently being studied in human clinical trials as a tamponade agent in retinal detachment surgery [48]. We report that SLIPS-modified ePTFE implants (ePTFE-SLIPS) limit bacterial adhesion without inhibiting macrophage viability or bactericidal activity. Significantly, in an animal model of device-associated infection, SLIPS-modified implants effectively resist *S. aureus* infection with a dramatic reduction in the magnitude of the innate immune response.

2. Materials and Methods

2.1 SLIPS fabrication and characterization

SLIPS were generated as previously described [30]. An ePTFE membrane with a 370 μm thickness and a 30 μm internodal distance was used (Aeos®, Zeus). The ePTFE membrane was cut into 6 mm diameter disks using a biopsy punch, sterilized with 70% ETOH for 30 min, and air dried for 20 min. Some of the dried disks were left untreated as controls. Three fluorinated lubricants were examined: perfluoropolyether (PFPE, Krytox ® GPL103, DuPont), perfluoroperhydro-phenanthrene (PFPH, FluoroMed), and perfluorodecalin (PFD, FluoroMed). All lubricants were filtered through 0.2 μm filter. PFPE and PFPH SLIPS lubricants were applied at a loading volume of 40 μL/cm^2. After allowing these liquids to diffuse into the ePTFE for 10 min, the disks were tilted for 5 min to remove excess liquid. For PFD-SLIPS, disks were submerged in the lubricant until saturated, then used within 1 min after removal to minimize evaporative losses.

A tilting water drop assay was used to determine the sliding angle. A 30 μL drop of deionized, distilled (DD) water was placed on the sample surface, and the sample slowly tilted upward until the droplet began to move. The minimum angle required for droplet movement was recorded. Each test was performed at least four times.

SLIPS stability in both air and PBS was monitored using an upright Zeiss LSM 710 confocal microscope in reflection mode. Samples were placed under a 10x air or liquid-immersion objective and exposed to 633 nm laser light, which was then collected as it reflected off the sample. A loss of lubricant could be monitored as a loss of reflected light. Samples were measured daily. The evaporation of the PFPE, PFPH, and PFD lubricants in air were also monitored gravimetrically using a standard laboratory microbalance (Mettler-Toledo) with reported repeatability of 0.1 mg. Masses were recorded every three minutes for PFD and every 15 min for PFPE and PFPH.

2.2. Bacterial adhesion

Staphylococcus aureus ATCC 12600 (strain NCTC8532) liquid stocks with a density of approximately 10^8 cell/mL were prepared in tryptic soy broth (TSB). This particular strain was chosen as it readily expresses virulence factors including protein A, coagulase, α-haemolysin, and δ-haemolysin and given that it is the source strain for PerkinElmer Xen29, the luciferase-transformed *S. aureus* strain that has been frequently utilized in similar implant studies [16, 49]. Control ePTFE or SLIPS coated ePTFE (ePTFE-SLIPS) samples (1 cm × 1 cm) were submerged in sterile biofilm medium (TSB with 1.5% (w/v) NaCl) and inoculated with 1:100 (v/v) of the *S. aureus* stock. The inoculated samples were then incubated for 48 h at 37°C. After the incubation period, samples were gently removed from the solution for SEM analysis and colony-forming units (CFUs) quantification. With regards to SEM analysis, samples were briefly rinsed to remove planktonic bacteria and serially dehydrated in increasing concentrations of EtOH and then dried in a Supercritical Autosamdri 815B critical point drier (Tousimis). The dehydrated samples were mounted, sputter-coated with Au/Pd, and imaged on a Zeiss Ultra Plus field emission SEM (Carl Zeiss). For CFU quantification, samples were washed three times in 10 mL of PBS by a gentle three second vortex to remove loosely associated bacteria. Next, to dislodge adherent bacteria, the washed samples were sonicated at 40 kHz in 1 mL of sterile PBS for three minutes and agitated on a vortex mixer for 90 seconds. This cycle of sonication and agitation was repeated four times. For quantitative culture, the PBS was serially diluted, plated on agar, cultured in 37°C 24 h, and the resultant colonies then counted. Of note, in order to study stability over time, ePTFE-SLIPS test samples were submerged in PBS or 50% rat serum for 1, 7, 14 and 21 day incubation periods after which samples were subsequently exposed to *S. aureus* and the aforementioned bacterial adhesion assay performed.

2.3 Macrophage adhesion, viability and activation on SLIPS

Primary macrophage isolation was performed in C57BL/6J male mice at maturity (8-12 weeks, Jackson Laboratory) according to a protocol approval by the Beth Israel Deaconess Institutional Animal Care and Use Committee. Sterile peritonitis was induced by intraperitoneal injection of 0.5 mL of 6% thioglycollate. Four days later, the peritoneal cavity was lavaged with 5 mL of 10 mM EDTA PBS to collect the elicited cells. Lavage

fluids were filtered using a 70 μm strainer and allowed to adhere to a petri-dish for 40 min. Unattached cells were removed and attached purified macrophages were lifted by non-enzymatic cell dissociation solution (Sigma-Aldrich) and counted using a hemocytometer.

Macrophage adhesion on SLIPS-modified samples was measured using a crystal violet based method, as described by Chamberlain et al[50]. Unmodified or SLIPS-modified 6 mm disks of ePTFE were placed in 96 well plates and five replicates were included in each group. The same approach was used for all in vitro macrophage assays, unless otherwise specified. Macrophages were seeded at 100,000 cells per well in 10% fetal bovine serum (FBS) in Dulbecco's Modified Eagle Medium (DMEM) for 1 h. Disks were washed with DMEM and fixed with 10% formalin for 10 min. After another wash, adherent cells were stained with crystal violet for 10 min and thoroughly washed with ddH_2O and dried in a vacuum desiccator. Remaining crystal violet was dissolved in 2% sodium dodecyl sulfate (SDS) and absorbance was measured at 540 nm. The absorbance was translated into cell number based on a standard curve.

To examine the effect of SLIPS on macrophage viability, macrophages were seeded at 60,000 cells per well for 12 h. A final concentration of 10% Alamar blue (Thermo Scientific) was added to the culture and incubated for 12 h. At the end of the 24 h culture, medium absorbance was measured at 570 nm and 610 nm from which the Alamar blue percent reduction was calculated following the manufacturer's instruction. Percent reduction was further converted to viable cell number using a standard curve.

The effect of SLIPS treatment on macrophage cytokine expression was investigated by seeding macrophages at 150,000 cells per well for 18 h. Total RNA was harvested with TRIzol (Invitrogen) and 0.1 μg of RNA was converted to cDNA using a high capacity cDNA reverse transcription kit (Invitrogen). qPCR was performed on the Applied Biosystems 7900 using TaqMan® Universal PCR Master Mix (Life Technologies) with TaqMan® primer against IL-1 β (Mm00434228_m1) and IL-6 (Mm00446190_m1). The fold increase from experimental groups to tissue culture plastic control was calculated using the delta-delta CT method with 18S (Mm00446186_m1, Life Technologies) as an internal reference gene.

2.4. Macrophage bactericidal and phagocytosis responses on SLIPS

To visualize macrophage phagocytosis of *S. aureus* on SLIPS treated samples, macrophages were stained with 3 μM of the blue dye, CellTrace Violet (C34557, Life Technology) and plated at 2×10^6 macrophages per well in a six well plate containing 35 mm diameter ePTFE or PFPE infused ePTFE disks. After a 24 h culture period, *S. aureus* was stained with 5 μM of the green dye Syto 9 (S-34854, Life Technology) and 50×10^6 bacteria were added to each well. After a 30 min co-culture period, plates were directly imaged by an Upright Zeiss LSM 710 confocal microscope with a 40x water immersion lens in reflection mode.

The effect of SLIPS on macrophage phagocytosis was quantified by flow cytometry using a protocol adopted from Gunther et al. [51] Briefly, macrophages and *S. aureus* were fluorescently stained, as described above. A total of 200,000 cells were seeded in each well for 24 h followed by the addition of 2×10^6 *S. aureus* to each culture. Experiments were performed at 37°C and 4°C. After a 1 h co-culture period, the disks were placed in cell

dissociation solution (20 mM EDTA, PBS) with constant agitation for 15 min at 4°C. Dissociated cell suspensions were examined by flow cytometry (LSRII, BD Bioscience). The intensity of the green bacterial signal that is associated with the blue macrophage signal was quantified. The specific phagocytosis signal was further calculated by subtracting the non-specific signal obtained at 4°C from the total signal measured at 37°C.

To examine the effect of SLIPS on bactericidal function of macrophages, a CFU based method was used, as described by Hanke et al. with modifications[52]. *S. aureus* were seeded at 2.5×10^3 CFU per well for 24 h at 4°C in DMEM medium supplied with 10% fetal bovine serum (not heat inactivated), which allows bacteria to settle and attach to the bottom of the well with restricted proliferation. A total of 250,000 macrophages were then aliquoted into the well and incubated for 1 h at 37°C. Several wells were also incubated without the addition of macrophages to serve as a control. Disks together with the culture medium were transported to 1 mL PBS and were subject to four cycles of shaking (1.5 min) and sonication (3 min) at 40 kHz to generate a single bacteria suspension. Mixtures were serially diluted and plated on agar plates for CFU counts.

2.5. Rat subcutaneous model of implant associated infection

All in vivo animal models were performed in male Wistar rats (200 gm, Charles River), according to a protocol approval by the Beth Israel Deaconess Institutional Animal Care and Use Committee. All animal protocols also comply with the NIH Guidelines for the Care and Use of Laboratory Animals. Subcutaneous implantation and subsequent bacteria injection were performed as described previously by Thurlow et al. with modifications [53]. Briefly, hair was removed from a 5 cm × 8 cm area from the upper back. Four disks of the same test group were surgically inserted into the subcutaneous tissue in each rat. Wounds were closed with sutures and staples. The precise location of the implant was marked on the skin surface. Using the skin mark as a guide, 24 h later, 2.6×10^7 CFU of *S. aureus* in 50 μL of PBS was injected subcutaneously. While the administered CFU exceed clinical relevance, the inoculation dose is in range with previously reported rodent foreign body infection models [5, 54-56]. A 24 h delay to inoculation was selected to decrease the confounding effect of the initial inflammatory response inherent to surgical manipulation [54, 57, 58]. Rats were euthanized 3 or 7 days after bacterial challenge and implants retrieved. At the time of explant, we confirmed that implants did not migrate from the previously marked skin site. Our described model resulted in an implant-driven, acute, reproducible infection that fully resolved within 10 days.

To quantify the bacterial burden, implants and surrounding tissue were surgically removed and the collected tissue sample was weighed by analytical balance. Both implant and tissue were minced. Sensitive broth culture was used to detect implant infection [5, 59-62]. Minced implants were sonicated in Luria-Bertani broth medium at 40 kHz for 5 min to detach bacteria and incubated at 37°C with shaking at 225 rpm for 20 h, as an amplification period to increase the sensitivity of bacterial detection [5, 60]. Broth turbidity was then measured by OD600 and the culture media was diluted and plated on agar to verify the presence of *S. aureus* CFUs. The implant was considered infected if the OD600 reading was above the lower detection limit of 0.02 and *S. aureus* was present on the agar plate. Infection rate (%)

was calculated by dividing the number of infected implants by the total number of implants. To quantify tissue bacterial burden, minced tissues were digested in 2 mg/mL of collagenase (Sigma-Aldrich) for 2 h with constant agitation at 37°C. The reaction was stopped by neutralizing with 10% FBS DMEM at 4°C. Digested cell suspensions were filtered through 70 μM cell strainers, diluted and plated on agar plates for CFU analysis.

Leukocyte cell density on implants and in surrounding tissues was quantified by extracting cells using the same collagenase protocol. Single cell suspensions were mixed with cell counting beads (X1272K, Exalpha) for flow cytometric determination of total cell number. Cell suspensions were co-stained with leukocyte CD45 antibody (561586, BD Pharmingen) together with either anti-macrophage antibody (554901, BD Pharmingen) or anti-neutrophil antibody (550002, BD Pharmingen) for flow cytometric determination of the leukocyte composition. Cell number was further normalized by tissue weight to calculate cell density.

To visualize infection and inflammation around the implants, histological analysis of tissue sections was performed. Tissue blocks were fixed overnight in 10% neutral buffered formalin and processed for paraffin embedding by Auotstainer XL (Leica). Embedded blocks were further sectioned at 5 μm thickness. To visualize *S. aureus*, sections were cleared in xylene and rehydrated through alcohol gradient and stained with tissue gram stain kit (HT90, Sigma-Aldrich) following the manufacturer's protocol. Briefly, sections were stained sequentially with crystal violet solution, Gram's Iodine, counterstained with safranin O and tartrazine solution separated by washing steps with alcohol and water and cleared in xylene for mounting. Tissue Gram stain was used to demonstrate the gross bacterial load rather than visualize individual bacteria morphology [53, 63]. To visualize the inflammatory response, hematoxylin and eosin staining (H&E) was performed. Briefly, sections were cleared with xylene, rehydrated through alcohol gradient, stained by Hematoxylin, washed by acid and ammonium alcohol, rinsed in water and exposed to Eosin followed by dehydrating through graded alcohols and cleared in xylene. All sections were mounted using Permount (Fisher Scientific) and visualized using BX41 microscope (Olympus) with a 4x or 20x objective lens. Microscale surface morphology of the retrieved implants was examined by SEM, as described above.

2.6. Host response to sterile subcutaneous implantation of SLIPS-treated samples

To examine the host response to unmodified or SLIPS-modified ePTFE implants in the absence of a bacterial challenge, the same implant procedure was conducted excluding bacterial inoculation. After a 7 day implant period, the entire implant and associated peri-implant tissue was surgically removed and processed, as described above. To quantify encapsulation thickness, sections were stained using Masson's Trichrome staining kit (HT15, Sigma-Aldrich), following the manufacturer's protocol. Capsule thickness was defined as thickness of the collagen connective tissue, stained blue, extending from the basal side or apical side of the implant. For each section, at least three measurements were obtained. Two to three sections from each implant were quantified to determine average capsule thickness. An average of five implants was quantified for each group.

2.7. Statistical analysis

Data are expressed as mean ± standard deviation (s.d.) in bar graphs or as a mean value in dot plots—Statistical differences were assessed using one-way ANOVA and post hoc testing performed using Bonferroni's modification of Student's *t* test for multiple comparisons (GraphPad Prism 5.0). Percentage difference was examined by chi-square test. A *p* value of less than 0.05 was considered statistically significant.

3. Results

3.1. SLIPS interfaces are stable in an aqueous environment and resist bacterial adhesion

ePTFE samples were readily modified with an immobilized fluorinated liquid overlayer to create a water-repellant SLIPS interface (ePTFE-SLIPS), as illustrated by a water droplet sliding angle assay. The tilt angle at which a water droplet begins to slide is 30° for unmodified ePTFE, but decreases to about 10° for SLIPS interfaces composed of PFPE and PFPH liquids and to about 5° when ePTFE was modified with PFD (Fig. 1A). The stability of the SLIPS lubricant layer in an aqueous environment was examined by submerging ePTFE-SLIPS samples in phosphate buffered saline (PBS). The uniformity of the SLIPS interface was assessed by confocal microscopy in reflection mode. In freshly prepared samples, a homogenous, defect free, bright field was observed caused by reflection of the incident laser light from the smooth liquid surface, which was unchanged after 1 week in PBS, regardless of the nature of the infused lubricant (PFPE, PFPH, PFD) (Fig. 1B). When ePTFE-SLIPS samples were incubated in air, surface loss of the most volatile fluorinated lubricant (PFD) was observed after 30 min, while PFPH and PFPE displayed greater stability (Fig. 1B and Supplementary Figure 1).

ePTFE-SLIPS samples were incubated with *S. aureus* for 48 h in bacteria growth media to assess their resistance to bacterial adhesion. After a brief rinse to remove planktonic bacteria, samples were fixed and initially examined by scanning electron microscopy (SEM). *S. aureus* aggregates were observed on unmodified ePTFE surfaces with few or no bacteria on SLIPS-modified samples (Fig. 1C). Adhered bacteria were detached via sonication, and a CFU assay was used to quantify surface adherent *S. aureus*, which demonstrate a 98.3%, 99.7%, and 99.1% reduction in bacterial adhesion for PFPE, PHPH and PFD coated surfaces, respectively (Fig. 1D, $p \leq 0.05$, n=6/group, one-way ANOVA and post hoc testing performed with Bonferroni's modification of Student *t* test for multiple comparisons). The functional stability of the SLIPS system in a physiological relevant environment over time was examined by incubating ePTFE and PFPE or PFPH coated ePTFE test samples in 50% rat serum for 1, 7, 14, and 21 days with subsequent exposure to *S. aureus* for two days. PFD was not included due to significant vaporization observed beyond 7 days of incubation, a finding consistent with its high vapor pressure. A similar 100-fold reduction in bacterial adhesion in PFPE and PFPH coated ePTFE samples was maintained over the 21 day exposure period (Fig. 1E). This experiment was also performed in PBS yielding comparable results (Supplementary Figure 2). These data demonstrate that a variety of fluorinated liquids, including PFPE, PFPH, and PFD can be incorporated into ePTFE as immobilized SLIPS interfaces with excellent physical and functional stability under aqueous conditions.

Moreover, despite prolonged exposure periods to bacteria in protein rich serum and growth media, SLIPS treatment significantly reduced *S. aureus* adhesion to ePTFE.

3.2. SLIPS-modified implants do not alter macrophage bactericidal activity

Macrophage adhesion, viability, phagocytosis, and bactericidal activity were examined on unmodified and SLIPS-modified ePTFE. Macrophage attachment after a 2 h incubation period was reduced by ~80% on all SLIPS substrates (Fig. 2A) with no impact observed on macrophage viability after a 24 h culture period on test samples (Fig. 2B). Macrophage phagocytosis was determined by co-incubating green fluorescent *S. aureus* with blue fluorescent macrophages cultured on unmodified or SLIPS-modified ePTFE disks. Phagocytosis of *S. aureus* was qualitatively observed on ePTFE-SLIPS after 30 min (Fig. 2C and Supplementary Figure 3) using confocal microscopy, suggesting that macrophages cultured on both SLIPS and unmodified ePTFE substrates displayed similar phagocytic activity. Flow cytometry was used to quantify macrophage bacterial uptake [51]. We observed no statistical difference between ePTFE and SLIPS-ePTFE, confirming that SLIPS coatings do not impact phagocytosis (Fig. 2D-E). Since viable *S. aureus* may persist after phagocytosis [64], the ability of macrophages to exert an effective bactericidal effect in the presence of a SLIPS-modified substrate was determined using a colony forming unit assay. A ~50% reduction in CFU was observed after exposure of macrophages to *S. aureus* for 1 h, which was similar on both SLIPS-modified and unmodified substrates (Fig. 2F). Although macrophage adhesion on SLIPS substrates is reduced, these data confirm that surface-immobilized fluorinated lubricants do not compromise macrophage viability or their ability to engulf or kill *S. aureus*.

3.3. ePTFE implants containing a SLIPS interface resist bacterial infection in vivo

A rat model of implant-associated bacterial infection was developed to evaluate the performance of SLIPS-modified implants in vivo. ePTFE or ePTFE-SLIPS test samples were implanted into the subcutaneous space and challenged 24 h later with injection of 2.6×10^7 CFU of *S. aureus* into the implant pocket. The inoculation dose was empirically determined to drive infection only in the presence of an implanted biomaterial. Implants and surrounding tissues were harvested three days after inoculation (Fig. 3A) [53]. The presence of bacteria was initially assessed by incubating retrieved samples in culture media and monitoring turbidity. *S. aureus* contamination was consistently observed for explanted ePTFE samples, but rarely in the case of SLIPS-treated implant. The infection rate was 92.3%, 33.3%, 0%, and 0% for ePTFE, PFPE, PFPH, and PFD, respectively ($p < 0.05$ vs. ePTFE, n≈9/group, chi-square test for significance; Fig. 3B). Similar results were observed from the OD600 measurement of culture broth (Supplementary Figure 4). Likewise, SEM imaging of explanted ePTFE samples, which had not been exposed to bacteria, revealed the presence of a fibrous surface matrix and occasional leukocytes (Fig. 3C). Upon bacterial challenge, fibrous matrix deposition was more pronounced and both leukocytes and aggregates of *S. aureus* were observed. Notably, all SLIPS-modified samples were free of matrix, cells, and bacteria with surface topography identical to that of pre-implant ePTFE (Fig. 3C and Supplementary Figure 5). Bacterial Gram staining confirmed strong staining at the ePTFE implant-tissue interface, which extended 100 μm from the implant surface (Fig. 3D and Supplementary Figure 6). ePTFE-SLIPS implants displayed limited staining for *S.*

aureus at the implant-tissue interface. In this acute infection model, unmodified ePTFE implants were culture free by 10 days.

Bacterial staining of the peri-implant tissue, approximately 500 μm away from the implant surface, demonstrated scattered bacteria in all test groups three days after *S. aureus* inoculation (Fig. 4A). Consistent with this observation, bacterial CFU/mg of peri-implant tissue was similar for all samples, including tissue harvested after bacterial challenge, but in the absence of an implanted material (Fig. 4B). At day 7, there were no detectable CFUs in animals that received *S. aureus* inoculation in the absence of implant. Day 7 bacterial persistence in the peri-implant host tissue was observed in 25% of unmodified implants, 10% for PFPE- and PFPH-modified surfaces, and 0% in PFD-modified implants (Fig. 4C-D), these results were not significant. Collectively, these data support that SLIPS modification specifically limits colonization at the implant surface.

3.4. SLIPS reduces the magnitude of the local inflammatory response

As evident three days after inoculation of *S. aureus,* bacterial challenge triggered an intense inflammatory response in the vicinity of unmodified ePTFE implants (Fig. 5 C,F). Notably, only a thin cellular infiltrate was observed immediately adjacent to all three SLIPS implant groups with only a mild level of immune cell infiltration within the peri-implant host tissue (Fig.5 G-L). A more limited inflammatory cell response was observed in the absence of bacterial inoculation (Fig.5 A,D) or in response to *S. aureus* challenge in the absence of an implant (Fig. 5B,E).

We used flow cytometry to quantify infiltration of $CD45^+$ leukocytes, macrophages, and neutrophils associated with *S. aureus* challenge to unmodified ePTFE and ePTFE-SLIPS implants. Results were compared to sterile ePTFE control, which illustrates a relatively mild inflammatory infiltration related to the host foreign body response (Fig. 5A, Fig. 6A-C, and Supplementary Figure 7). At the implant surface, we observe a significantly elevated inflammatory response in unmodified ePTFE that has been challenged with *S. aureus*. This is consistent with *S. aureus* adhesion and inflammatory abscess formation around ePTFE implants (Fig. 5C and Fig. 6A-C). We observe a 90% reduction in leukocyte response to *S. aureus* challenged ePTFE-SLIPS implants, consistent with our hypothesis that SLIPS lubricants prevent *S. aureus* adhesion and subsequent abscess formation (Fig. 6A-C). Peri-implant tissue inflammation was also quantified using flow cytometry; controls included both unmodified, sterile ePTFE and *S. aureus* only (no implant) enrollment. Consistent with inflammatory responses quantified at the implant surface, we observe significantly elevated leukocyte infiltration in tissue surrounding the *S. aureus* challenged ePTFE implant. Tissue leukocyte presence was reduced 50% in *S. aureus* challenged ePTFE-SLIPS, equivalent to tissue inflammation observed with sterile ePTFE and *S. aureus* only enrollment (Fig. 6D-F). Significantly, these results suggest that the material-associated infection is driving the immune response.

3.5. SLIPS reduces capsule thickness in a sterile implant model

SLIPS biocompatibility and stability were evaluated in a sterile subcutaneous implant model. One week after implantation, the presence of a SLIPS interface reduced capsule

thickness by ~50% both from the basal side (Fig. 7A, B) and the apical side (Supplementary Figure 8) without discernible loss of the fluorinated SLIPS lubricant (Supplementary Figure 9). Macrophages are largely responsible for orchestrating the host foreign body response by release of inflammatory mediators, such as IL-1β and IL-6 [65]. Indeed, exposure of macrophages to ePTFE alone upregulated IL-1β and IL-6 expression by ~60- and ~12-fold, respectively (Fig. 7C, D). In contrast, IL-1β and IL-6 expression were reduced by 80% and 60%, respectively, when macrophages were cultured on SLIPS-treated implants. These data suggest that SLIPS may limit the encapsulation response by attenuating macrophage activation.

4. Discussion

Over half of the 1.7 million annual nosocomial infections in the US are device-associated, resulting from surface colonization by microbes [66]. Intra- and extracorporeal synthetic biomaterials, such as those used for urinary and vascular catheters, prosthetic vascular grafts and mesh materials, as well as hemodialysis systems are all prone to biofouling. The development of a device-associated infection can be attributed to the propensity of bacteria to form biofilms on all currently available biomaterials, as well as the capacity of a foreign material itself to impair local innate immune responses [67, 68]. Together, the presence of a biofilm and impaired local host defense mechanisms facilitate bacterial colonization and infection in the peri-implant tissue [3-5, 69, 70]. Current methods to combat biofouling include schemes to prevent nonspecific protein and cell adhesion or strategies for the presentation or elution of bactericidal agents. However, the inability to identify a unique set of physiochemical features that afford a truly non-adhesive film, the broad range of anti-microbial sensitivities among microorganisms, and the finite capacity of drug reservoirs continue to limit these approaches.

To date, SLIPS have been fabricated on a variety of substrates [32, 71, 72] by incorporation of an immobilized liquid interface, which is omniphobic across a broad range of temperature, pressure, surface tension, and other conditions [29]. SLIPS-based surfaces are stable when exposed to UV or ethylene oxide, as conditions for device sterilization, and are low-cost, passive, and simple to manufacture [30]. Data in this study and in a prior report demonstrate that immobilized liquid interfaces are highly resistant to bacterial adhesion[30], presumably because the liquid interface is difficult for microorganisms to adhere and penetrate, even with bacterial surfactant production. Without access to the solid material beneath a SLIPS liquid, bacteria are unable to attach, and are thus subject to passive removal.

This report is the first to demonstrate that an immobilized water-immiscible liquid layer serves not only to limit biofouling in an ambient environment, but also to impede infection in a rodent implant model. To examine the performance of SLIPS systems in vivo, ePTFE mesh was selected as a model implant material. Microporous hydrophobic implants, such as those made of ePTFE, are widely used clinically but are particularly susceptible to bacterial infection [44, 45]. SLIPS modification was easily achieved by infusing ePTFE with a number of fluorinated liquids, including PFPH which has been tested clinically [46] and PFD which is currently undergoing human clinical trials [48]. Remarkably, SLIPS masked

conventional biomaterial niches that facilitate bacterial persistence and proliferation in vivo, without compromising macrophage phagocytosis or bacterial killing in vitro. As cultured neutrophils are extremely sensitive to activation and spontaneous apoptosis, we chose to focus in vitro studies on macrophages. In vivo, we observe both neutrophils and macrophages participating in the host response to resolve *S. aureus* from ePTFE-SLIPS implant pockets. Therefore, a SLIPS system enables bacterial elimination in the region of the implant and does so in the context of a substantially lower innate immune response. We anticipate that this technology will provide an important strategy to reduce the risk of device-associated infection along with the attendant morbidity and mortality associated with these complications.

In addition to diminishing the propensity of device-associated bacterial infection, SLIPS-modified implants also displayed a marked reduction in inflammatory capsule formation at early time points. Specifically, as our study was limited to a seven-day characterization, we do not capture the full evolution of capsule formation but our results suggest that early host foreign body response is significantly reduced with SLIPS coating. Previous reports have shown that encapsulation of implants is related to macrophage activation [73, 74]. In this regard, the induction of a thinner fibrous capsule by SLIPS-treated materials may be related both to a reduction in the magnitude of the peri-implant inflammatory response and a lower level macrophage activation, as measured by decreased expression of IL-1β and IL-6 [74, 75].

The SLIPS system described in this report was designed for use on permanent implants and primarily functions as a non-adhesive coating. As such, it was designed to prevent bacterial adhesion and biofilm attachment that occurs in the acute period following surgical intervention and does not facilitate tissue integration given concerns that surfaces favoring host cell adhesion promote attachment of microorganisms that use similar mechanisms for adsorption [76]. The inability to simultaneously promote tissue integration while reducing the risk of device infection may be a limitation of the current technology. Indeed, the “race for the surface” paradigm, which describes the competition between cell integration and bacterial adhesion to implant surfaces, emphasizes the critical importance of establishing immunocompetent host integration before microbial colonization for long term implant success [12, 76]. Multifunctional surfaces that promote host cell adhesion while simultaneously antagonizing microbial attachment remain a challenge to the biomaterials community. SLIPS coatings can be tailored to provide either acute or long term stability and, although not a focus of the current report, SLIPS coatings provide both anti-microbial and anti-thrombotic functionality [35] and, therefore, perform in the desirable class of next-generation, multi-functional surfaces. SLIPS stability over an acute course (weeks) following surgical implantation may be the most desirable application. This would provide immediate protection from microbial colonization and, over the desired timeline, the surface would evolve to allow host integration and long term immunocompetence. The inherent stability of a surface bound SLIPS liquid is dependent upon the extent of physical entrapment within the porous substrate and the chemical affinity between the liquid and solid. Although fluorinated liquids are all immiscible in water, vapor pressure may vary widely. For example, perfluorodecalin has a high vapor pressure and, when injected intravenously as an oxygen carrier, displays a half-life of less than 24 h [77]. Indeed, when

PFD-based SLIPS implants were stored in air, the infused liquid was largely lost within 1 h. However, once placed within a closed subcutaneous space, the PFD liquid layer remained intact throughout the implantation period. This observation is consistent with that of similar test samples incubated in PBS in vitro, as well as with prior reports of SLIPS surfaces in direct contact with blood under physiologic flow conditions [78]. SLIPS systems, derived from the fluorinated liquids, PFPH and PFPE, contain surface liquid layers with intrinsically lower vapor pressures, and greater viscosities. These systems displayed enhanced persistence of the surface-bound liquid in open air. While little difference was noted among the various SLIPS systems at the time of implant retrieval on days 3 and 7, presumably those systems based on PFPH and PFPE would exhibit extended in vivo durability compared to PFD due to reduced vapor pressure. This is supported by the extended stability assay in vitro, where PFPH and PFPE coated implants resist bacterial adhesion for incubation periods of at least 21 days. Although not addressed in the current study, in principle, a liquid could be selected to reduce the likelihood of device-associated bacterial infection immediately following surgical implantation, while subsequently dissipating to allow tissue integration at a later time point. Lastly, although additional studies are necessary, it is likely that the effect of reduced biofilm attachment noted with *S. aureus* in vivo may extend to additional bacterial species, as it has previously been demonstrated that in static and physiologic flow conditions in vitro, SLIPS surfaces significantly reduce *Pseudomonas aeruginosa* and *Escherichia coli* biofilm attachment by approximately 35 fold [30].

A recent study has reported that a tethered liquid perfluorocarbon (TLP) surface could prevent thrombus formation in a pig arteriovenous shunt model for up to 8 hours [35]. In this system, a PFC lubricant was incorporated as a liquid layer within a surface-tethered ultrathin perfluorinated polymer film bound to a non-porous polymer substrate. The current study is the first to characterize SLIPS-modified implants for extended periods in vivo and is the first to demonstrate the capacity of SLIPS to significantly limit the risk of device associated bacterial colonization and implant infection in vivo. Although ePTFE-SLIPS implant surfaces resolved *S. aureus* infection by day 3, we did observe some persistence of *S. aureus* in peri-implant tissue up to day 7. This observation is consistent with recent reports that suggest peri-implant tissue can serve as a niche for infection and perhaps create a chronic threat to implant sterility [70]. Broekhuizen et al. used a mouse model of *S. epidermidis* biomaterial-associated infection and observed that as post-implant inocula dose increased, peri-implant tissue was more often infected than silicon elastomer implant surfaces [5]. In a follow up study, Riool et al. examined the capacity of pre-established *S. epidermidis* implant (titanium or silicone elastomer) colonization to spread to peri-implant tissue. At 4 days post-implantation, the authors observed a high incidence of culture positive peri-implant tissue and consistent co-localization with macrophages [79]. Because mouse model, inoculum strain, and material implant properties all dictate the prevalence of tissue or material colonization, it can be difficult to correlate these *S. epidermidis* studies with our *S. aureus* ePTFE implant model. However, persistent colonization of peri-implant tissue would certainly pose an extended threat to implant sterility. Several recent approaches have reported the ability to impart anti-bacterial activity to biomaterials in vivo in long term studies, however these strategies have required the chemical modification of existing materials or the design of completely novel materials with an attendant need to fully define

the clinical safety and efficacy profile [14, 16]. The SLIPS systems used in this study were easily generated by combining clinically approved materials without a requirement for further modification. Thus, in practice ePTFE materials can undergo sterilization prior to coating and can be stored dry prior to implantation. Ideally, the graft material will be packaged with a SLIPS lubricant, which can then be applied either directly or by submersion in the operating room, as this process typically only takes minutes and can be performed during the procedure after the exact size and shape of the graft to be implanted is decided upon by the surgical team. In these circumstances, the shelf life would be on the order of years, as each component would be separately prepared and packaged. It should be noted that ePTFE membranes were employed in this study due to their frequent use in the clinical setting and their potential for secondary infection [44, 45]. However, SLIPS can also be fabricated on other common biomaterials, including non-porous arcrylic or polysulfone substrates after covalent binding of a tethered perfluorocarbon with subsequent infusion of a liquid perflurodecalin [35]; polydimethylsiloxane (PDMS) infused with silicone oil [34]; and steel surfaces after electrodeposition of nanoporous tungsten oxide coating, surface modification with a perfluroalkyl-bearing phosphate, and infusion with a fluorinated perfluropolyether lubricant [80].

5. Conclusion

Immobilized slippery liquid coating of medical devices provides a novel strategy for preventing bacterial adhesion and device infection. The studies reported herein demonstrate that SLIPS can be generated by infusing medical material ePTFE with clinically relevant perflurocabron liquids. The SLIPS modified material prevents bacterial attachment while preserving the viability and bactericidal function of macrophage in vitro. Upon implantation in vivo, SLIPS limits bacterial manifestation on the surface of implant and largely reduces local inflammation. In case of sterile implantation, SLIPS modification results in a beneficial thinner fibrous capsule likely due to a reduced macrophage inflammatory cytokine secretion. As demonstrated herein, SLIPS presents a promising technology that may have a transformative impact in reducing the risk of device-associated infection.

Supplementary Material

Refer to Web version on PubMed Central for supplementary material.

Acknowledgements

The authors acknowledge support from the Defense Advanced Research Projects Agency Grant N66001-11-1-4180 and Contract HR0011-13-C-0025. This work was also in part funded by NIH T32 HL 008843-21A1 and the American College of Surgeons Resident Research Scholarship to Madhukar S. Patel as well as NIH T35 HL 110843 to Katherine A. Moravec. We thank the members of the Dr. Chaikof and Dr. Aizenberg lab for helpful discussions, as well as Jaakko Timonen and Thomas Ferrante for confocal microscopy assistance. We also thank the research and animal facilities at BIDMC and the Wyss Institute.

References

1. Magill SS, Edwards JR, Bamberg W, Beldavs ZG, Dumyati G, Kainer MA, Lynfield R, Maloney M, McAllister-Hollod L, Nadle J, Ray SM, Thompson DL, Wilson LE, Fridkin SK. Multistate point-

prevalence survey of health care-associated infections. N Engl J Med. 2014; 370(13):1198–208. [PubMed: 24670166]

2. Virden CP, Dobke MK, Stein P, Parsons CL, Frank DH. Subclinical infection of the silicone breast implant surface as a possible cause of capsular contracture. Aesthetic Plast Surg. 1992; 16(2):173–9. [PubMed: 1570781]
3. Boelens JJ, Zaat SA, Murk JL, Weening JJ, van Der Poll T, Dankert J. Enhanced susceptibility to subcutaneous abscess formation and persistent infection around catheters is associated with sustained interleukin-1beta levels. Infect Immun. 2000; 68(3):1692–5. [PubMed: 10678990]
4. Vuong C, Kocianova S, Yao Y, Carmody AB, Otto M. Increased colonization of indwelling medical devices by quorum-sensing mutants of staphylococcus epidermidis in vivo. J Infect Dis. 2004; 190(8):1498–505. [PubMed: 15378444]
5. Broekhuizen CA, de Boer L, Schipper K, Jones CD, Quadir S, Feldman RG, Dankert J, Vandenbroucke-Grauls CM, Weening JJ, Zaat SA. Peri-implant tissue is an important niche for staphylococcus epidermidis in experimental biomaterial-associated infection in mice. Infect Immun. 2007; 75(3):1129–36. [PubMed: 17158900]
6. Stewart PS, Franklin MJ. Physiological heterogeneity in biofilms. Nat Rev Microbiol. 2008; 6(3): 199–210. [PubMed: 18264116]
7. Drenkard E, Ausubel FM. Pseudomonas biofilm formation and antibiotic resistance are linked to phenotypic variation. Nature. 2002; 416(6882):740–3. [PubMed: 11961556]
8. Mah TF, Pitts B, Pellock B, Walker GC, Stewart PS, O'Toole GA. A genetic basis for pseudomonas aeruginosa biofilm antibiotic resistance. Nature. 2003; 426(6964):306–10. [PubMed: 14628055]
9. Jesaitis AJ, Franklin MJ, Berglund D, Sasaki M, Lord CI, Bleazard JB, Duffy JE, Beyenal H, Lewandowski Z. Compromised host defense on pseudomonas aeruginosa biofilms: Characterization of neutrophil and biofilm interactions. J Immunol. 2003; 171(8):4329–39. [PubMed: 14530358]
10. Bjarnsholt T, Jensen PO, Burmolle M, Hentzer M, Haagensen JA, Hougen HP, Calum H, Madsen KG, Moser C, Molin S, Hoiby N, Givskov M. Pseudomonas aeruginosa tolerance to tobramycin, hydrogen peroxide and polymorphonuclear leukocytes is quorum-sensing dependent. Microbiology. 2005; 151(Pt 2):373–83. [PubMed: 15699188]
11. Epstein AK, Pokroy B, Seminara A, Aizenberg J. Bacterial biofilm shows persistent resistance to liquid wetting and gas penetration. Proc Natl Acad Sci U S A. 2011; 108(3):995–1000. [PubMed: 21191101]
12. Gristina AG. Biomaterial-centered infection: Microbial adhesion versus tissue integration. Science. 1987; 237(4822):1588–95. [PubMed: 3629258]
13. Jiang S, Cao Z. Ultralow-fouling, functionalizable, and hydrolyzable zwitterionic materials and their derivatives for biological applications. Advanced materials. 2010; 22(9):920–32. [PubMed: 20217815]
14. Smith RS, Zhang Z, Bouchard M, Li J, Lapp HS, Brotske GR, Lucchino DL, Weaver D, Roth LA, Coury A, Biggerstaff J, Sukavaneshvar S, Langer R, Loose C. Vascular catheters with a nonleaching poly-sulfobetaine surface modification reduce thrombus formation and microbial attachment. Science translational medicine. 2012; 4(153):153ra132.
15. Autumn K, Sitti M, Liang YA, Peattie AM, Hansen WR, Sponberg S, Kenny TW, Fearing R, Israelachvili JN, Full RJ. Evidence for van der waals adhesion in gecko setae. Proc Natl Acad Sci U S A. 2002; 99(19):12252–6. [PubMed: 12198184]
16. Hook AL, Chang CY, Yang J, Luckett J, Cockayne A, Atkinson S, Mei Y, Bayston R, Irvine DJ, Langer R, Anderson DG, Williams P, Davies MC, Alexander MR. Combinatorial discovery of polymers resistant to bacterial attachment. Nat Biotechnol. 2012; 30(9):868–75. [PubMed: 22885723]
17. Park KD, Kim YS, Han DK, Kim YH, Lee EH, Suh H, Choi KS. Bacterial adhesion on peg modified polyurethane surfaces. Biomaterials. 1998; 19(7-9):851–9. [PubMed: 9663762]
18. Prime KL, Whitesides GM. Self-assembled organic monolayers: Model systems for studying adsorption of proteins at surfaces. Science. 1991; 252(5009):1164–7. [PubMed: 2031186]
19. Brzozowska AM, de Keizer A, Detrembleur C, Cohen Stuart MA, Norde W. Grafted ionomer complexes and their effect on protein adsorption on silica and polysulfone surfaces. Colloid Polym Sci. 2010; 288(16-17):1621–1632. [PubMed: 21125002]

20. Banerjee I, Pangule RC, Kane RS. Antifouling coatings: Recent developments in the design of surfaces that prevent fouling by proteins, bacteria, and marine organisms. Advanced materials. 2011; 23(6):690–718. [PubMed: 20886559]
21. Zhao L, Chu PK, Zhang Y, Wu Z. Antibacterial coatings on titanium implants, Journal of biomedical materials research. Part B, Applied biomaterials. 2009; 91(1):470–80.
22. Chongsiriwatana NP, Patch JA, Czyzewski AM, Dohm MT, Ivankin A, Gidalevitz D, Zuckermann RN, Barron AE. Peptoids that mimic the structure, function, and mechanism of helical antimicrobial peptides. Proc Natl Acad Sci U S A. 2008; 105(8):2794–9. [PubMed: 18287037]
23. Costerton JW, Stewart PS, Greenberg EP. Bacterial biofilms: A common cause of persistent infections. Science. 1999; 284(5418):1318–22. [PubMed: 10334980]
24. Hall-Stoodley L, Costerton JW, Stoodley P. Bacterial biofilms: From the natural environment to infectious diseases, Nature reviews. Microbiology. 2004; 2(2):95–108. [PubMed: 15040259]
25. Fadeeva E, Truong VK, Stiesch M, Chichkov BN, Crawford RJ, Wang J, Ivanova EP. Bacterial retention on superhydrophobic titanium surfaces fabricated by femtosecond laser ablation. Langmuir. 2011; 27(6):3012–9. [PubMed: 21288031]
26. Genzer J, Efimenko K. Recent developments in superhydrophobic surfaces and their relevance to marine fouling: A review. Biofouling. 2006; 22(5-6):339–60. [PubMed: 17110357]
27. Tuteja A, Choi W, Mabry JM, McKinley GH, Cohen RE. Robust omniphobic surfaces. Proc Natl Acad Sci U S A. 2008; 105(47):18200–5. [PubMed: 19001270]
28. Bos R, van der Mei HC, Gold J, Busscher HJ. Retention of bacteria on a substratum surface with micro-patterned hydrophobicity. FEMS Microbiol Lett. 2000; 189(2):311–5. [PubMed: 10930757]
29. Wong TS, Kang SH, Tang SK, Smythe EJ, Hatton BD, Grinthal A, Aizenberg J. Bioinspired self-repairing slippery surfaces with pressure-stable omniphobicity. Nature. 2011; 477(7365):443–7. [PubMed: 21938066]
30. Epstein AK, Wong TS, Belisle RA, Boggs EM, Aizenberg J. Liquid-infused structured surfaces with exceptional anti-biofouling performance. Proc Natl Acad Sci U S A. 2012; 109(33):13182–7. [PubMed: 22847405]
31. Bohn HF, Federle W. Insect aquaplaning: Nepenthes pitcher plants capture prey with the peristome, a fully wettable water-lubricated anisotropic surface. Proc Natl Acad Sci U S A. 2004; 101(39): 14138–43. [PubMed: 15383667]
32. Kim P, Wong TS, Alvarenga J, Kreder MJ, Adorno-Martinez WE, Aizenberg J. Liquid-infused nanostructured surfaces with extreme anti-ice and anti-frost performance. ACS Nano. 2012; 6(8): 6569–77. [PubMed: 22680067]
33. Shillingford C, MacCallum N, Wong TS, Kim P, Aizenberg J. Fabrics coated with lubricated nanostructures display robust omniphobicity. Nanotechnology. 2014; 25(1):014019. [PubMed: 24334333]
34. Howell C, Vu TL, Lin JJ, Kolle S, Juthani N, Watson E, Weaver JC, Alvarenga J, Aizenberg J. Self-replenishing vascularized fouling-release surfaces. ACS Appl Mater Interfaces. 2014; 6(15): 13299–307. [PubMed: 25006681]
35. Leslie DC, Waterhouse A, Berthet JB, Valentin TM, Watters AL, Jain A, Kim P, Hatton BD, Nedder A, Donovan K, Super EH, Howell C, Johnson CP, Vu TL, Bolgen DE, Rifai S, Hansen AR, Aizenberg M, Super M, Aizenberg J, Ingber DE. A bioinspired omniphobic surface coating on medical devices prevents thrombosis and biofouling. Nat Biotechnol. 2014; 32(11):1134–40. [PubMed: 25306244]
36. Furnee E, Hazebroek E. Mesh in laparoscopic large hiatal hernia repair: A systematic review of the literature. Surg Endosc. 2013; 27(11):3998–4008. [PubMed: 23793804]
37. Robin-Lersundi A, Vega Ruiz V, Lopez-Monclus J, Cruz Cidoncha A, Abella Alvarez A, Melero Montes D, Blazquez Hernando L, Garcia-Urena MA. Temporary abdominal closure with polytetrafluoroethylene prosthetic mesh in critically ill non-trauma patients. Hernia. 2015; 19(2): 329–37. [PubMed: 24916420]
38. Cevasco M, Itani KM. Ventral hernia repair with synthetic, composite, and biologic mesh: Characteristics, indications, and infection profile. Surg Infect (Larchmt). 2012; 13(4):209–15. [PubMed: 22913337]

39. van der Slegt J, Steunenberg SL, Donker JM, Veen EJ, Ho GH, de Groot HG, van der Laan L. The current position of precuffed expanded polytetrafluoroethylene bypass grafts in peripheral vascular surgery. J Vasc Surg. 2014; 60(1):120–8. [PubMed: 24629990]
40. Yamashita E, Yamagishi M, Miyazaki T, Maeda Y, Yamamoto Y, Kato N, Asada S, Hongu H, Yaku H. Smaller-sized expanded polytetrafluoroethylene conduits with a fan-shaped valve and bulging sinuses for right ventricular outflow tract reconstruction. Ann Thorac Surg. 2016
41. Shadfar S, Farag A, Jarchow AM, Shockley WW. Safety and efficacy of expanded polytetrafluoroethylene implants in the surgical management of traumatic nasal deformity. JAMA Otolaryngol Head Neck Surg. 2015; 141(8):710–5. [PubMed: 26110468]
42. Godin MS, Waldman SR, Johnson CM Jr. The use of expanded polytetrafluoroethylene (gore-tex) in rhinoplasty. A 6-year experience. Arch Otolaryngol Head Neck Surg. 1995; 121(10):1131–6. [PubMed: 7546580]
43. Wong JK. Forehead augmentation with alloplastic implants. Facial Plast Surg Clin North Am. 2010; 18(1):71–7. [PubMed: 20206091]
44. Petersen S, Henke G, Freitag M, Faulhaber A, Ludwig K. Deep prosthesis infection in incisional hernia repair: Predictive factors and clinical outcome. Eur J Surg. 2001; 167(6):453–7. [PubMed: 11471671]
45. Deneuville M. Infection of ptfe grafts used to create arteriovenous fistulas for hemodialysis access. Ann Vasc Surg. 2000; 14(5):473–9. [PubMed: 10990557]
46. Kertes PJ, Wafapoor H, Peyman GA, Calixto N Jr. Thompson H. The management of giant retinal tears using perfluoroperhydrophenanthrene. A multicenter case series. Vitreon collaborative study group. Ophthalmology. 1997; 104(7):1159–65. [PubMed: 9224470]
47. Castro CI, Briceno JC. Perfluorocarbon-based oxygen carriers: Review of products and trials. Artif Organs. 2010; 34(8):622–34. [PubMed: 20698841]
48. Double endotamponade with perfluorodecalin and silicone oil in retinal detachment surgery. Https://clinicaltrials.Gov/show/nct01959568
49. Gemmell CG, Ford CW. Virulence factor expression by gram-positive cocci exposed to subinhibitory concentrations of linezolid. J Antimicrob Chemother. 2002; 50(5):665–72. [PubMed: 12407122]
50. Chamberlain LM, Godek ML, Gonzalez-Juarrero M, Grainger DW. Phenotypic non-equivalence of murine (monocyte−) macrophage cells in biomaterial and inflammatory models. J Biomed Mater Res A. 2009; 88(4):858–71. [PubMed: 18357567]
51. Gunther F, Wabnitz GH, Stroh P, Prior B, Obst U, Samstag Y, Wagner C, Hansch GM. Host defence against staphylococcus aureus biofilms infection: Phagocytosis of biofilms by polymorphonuclear neutrophils (pmn). Mol Immunol. 2009; 46(8-9):1805–13. [PubMed: 19261332]
52. Hanke ML, Heim CE, Angle A, Sanderson SD, Kielian T. Targeting macrophage activation for the prevention and treatment of staphylococcus aureus biofilm infections. J Immunol. 2013; 190(5): 2159–68. [PubMed: 23365077]
53. Thurlow LR, Hanke ML, Fritz T, Angle A, Aldrich A, Williams SH, Engebretsen IL, Bayles KW, Horswill AR, Kielian T. Staphylococcus aureus biofilms prevent macrophage phagocytosis and attenuate inflammation in vivo. J Immunol. 2011; 186(11):6585–96. [PubMed: 21525381]
54. Kuklin NA, Pancari GD, Tobery TW, Cope L, Jackson J, Gill C, Overbye K, Francis KP, Yu J, Montgomery D, Anderson AS, McClements W, Jansen KU. Real-time monitoring of bacterial infection in vivo: Development of bioluminescent staphylococcal foreign-body and deep-thigh-wound mouse infection models. Antimicrob Agents Chemother. 2003; 47(9):2740–8. [PubMed: 12936968]
55. Rupp ME, Ulphani JS, Fey PD, Bartscht K, Mack D. Characterization of the importance of polysaccharide intercellular adhesin/hemagglutinin of staphylococcus epidermidis in the pathogenesis of biomaterial-based infection in a mouse foreign body infection model. Infect Immun. 1999; 67(5):2627–32. [PubMed: 10225932]
56. Chen R, Willcox MD, Ho KK, Smyth D, Kumar N. Antimicrobial peptide melimine coating for titanium and its in vivo antibacterial activity in rodent subcutaneous infection models. Biomaterials. 2016; 85:142–51. [PubMed: 26871890]

57. Svensson S, Trobos M, Hoffman M, Norlindh B, Petronis S, Lausmaa J, Suska F, Thomsen P. A novel soft tissue model for biomaterial-associated infection and inflammation - bacteriological, morphological and molecular observations. Biomaterials. 2015; 41:106–21. [PubMed: 25522970]
58. Broughton G 2nd, Janis JE, Attinger CE. The basic science of wound healing. Plast Reconstr Surg. 2006; 117(7 Suppl):12S–34S. [PubMed: 16799372]
59. Atkins BL, Athanasou N, Deeks JJ, Crook DW, Simpson H, Peto TE, McLardy-Smith P, Berendt AR. Prospective evaluation of criteria for microbiological diagnosis of prosthetic-joint infection at revision arthroplasty. The osiris collaborative study group. J Clin Microbiol. 1998; 36(10):2932–9. [PubMed: 9738046]
60. Pajkos A, Deva AK, Vickery K, Cope C, Chang L, Cossart YE. Detection of subclinical infection in significant breast implant capsules. Plast Reconstr Surg. 2003; 111(5):1605–11. [PubMed: 12655204]
61. Carbonell AM, Matthews BD, Dreau D, Foster M, Austin CE, Kercher KW, Sing RF, Heniford BT. The susceptibility of prosthetic biomaterials to infection. Surg Endosc. 2005; 19(3):430–5. [PubMed: 15580439]
62. Schafer P, Fink B, Sandow D, Margull A, Berger I, Frommelt L. Prolonged bacterial culture to identify late periprosthetic joint infection: A promising strategy. Clin Infect Dis. 2008; 47(11): 1403–9. [PubMed: 18937579]
63. Lindner HB, Zhang A, Eldridge J, Demcheva M, Tsichlis P, Seth A, Vournakis J, Muise-Helmericks RC. Anti-bacterial effects of poly-n-acetyl-glucosamine nanofibers in cutaneous wound healing: Requirement for akt1. PLoS One. 2011; 6(4):e18996. [PubMed: 21559496]
64. Kubica M, Guzik K, Koziel J, Zarebski M, Richter W, Gajkowska B, Golda A, Maciag-Gudowska A, Brix K, Shaw L, Foster T, Potempa J. A potential new pathway for staphylococcus aureus dissemination: The silent survival of s. Aureus phagocytosed by human monocyte-derived macrophages. PLoS One. 2008; 3(1):e1409. [PubMed: 18183290]
65. Anderson JM, Rodriguez A, Chang DT. Foreign body reaction to biomaterials. Semin Immunol. 2008; 20(2):86–100. [PubMed: 18162407]
66. Scott, RD. The direct medical costs of healthcare-associated infections in u.S. Hospitals and the benefits of prevention. Center for Disease Control and Prevention; 2009.
67. Zimmerli W, Lew PD, Waldvogel FA. Pathogenesis of foreign body infection. Evidence for a local granulocyte defect. J Clin Invest. 1984; 73(4):1191–200. [PubMed: 6323536]
68. Zimmerli W, Sendi P. Pathogenesis of implant-associated infection: The role of the host. Semin Immunopathol. 2011; 33(3):295–306. [PubMed: 21603890]
69. Boelens JJ, Zaat SA, Meeldijk J, Dankert J. Subcutaneous abscess formation around catheters induced by viable and nonviable staphylococcus epidermidis as well as by small amounts of bacterial cell wall components. J Biomed Mater Res. 2000; 50(4):546–56. [PubMed: 10756313]
70. Broekhuizen CA, Schultz MJ, van der Wal AC, Boszhard L, de Boer L, Vandenbroucke-Grauls CM, Zaat SA. Tissue around catheters is a niche for bacteria associated with medical device infection. Crit Care Med. 2008; 36(8):2395–402. [PubMed: 18664789]
71. Kim P, Kreder MJ, Alvarenga J, Aizenberg J. Hierarchical or not? Effect of the length scale and hierarchy of the surface roughness on omniphobicity of lubricant-infused substrates. Nano Lett. 2013; 13(4):1793–9. [PubMed: 23464578]
72. Vogel N, Belisle RA, Hatton B, Wong TS, Aizenberg J. Transparency and damage tolerance of patternable omniphobic lubricated surfaces based on inverse colloidal monolayers. Nat Commun. 2013; 4:2167.
73. Salzmann DL, Kleinert LB, Berman SS, Williams SK. The effects of porosity on endothelialization of eptfe implanted in subcutaneous and adipose tissue. J Biomed Mater Res. 1997; 34(4):463–76. [PubMed: 9054530]
74. Bota PC, Collie AM, Puolakkainen P, Vernon RB, Sage EH, Ratner BD, Stayton PS. Biomaterial topography alters healing in vivo and monocyte/macrophage activation in vitro. J Biomed Mater Res A. 2010; 95(2):649–57. [PubMed: 20725970]
75. Bonfield TL, Colton E, Anderson JM. Plasma protein adsorbed biomedical polymers: Activation of human monocytes and induction of interleukin 1. J Biomed Mater Res. 1989; 23(6):535–48. [PubMed: 2786877]

76. Busscher HJ, van der Mei HC, Subbiahdoss G, Jutte PC, van den Dungen JJ, Zaat SA, Schultz MJ, Grainger DW. Biomaterial-associated infection: Locating the finish line in the race for the surface. Sci Transl Med. 2012; 4(153):153rv10.

77. Spahn DR. Blood substitutes. Artificial oxygen carriers: Perfluorocarbon emulsions. Crit Care. 1999; 3(5):R93–7. [PubMed: 11094488]

78. Howell C, Vu TL, Johnson CP, Hou X, Ahanotu O, Alvarenga J, Leslie DC, Uzun O, Waterhouse A, Kim P, Super M, Aizenberg M, Ingber DE, Aizenberg J. Stability of surface-immobilized lubricant interfaces under flow. Chemistry of Materials. 2015; 27(5):1792–1800.

79. Riool M, de Boer L, Jaspers V, van der Loos CM, van Wamel WJ, Wu G, Kwakman PH, Zaat SA. Staphylococcus epidermidis originating from titanium implants infects surrounding tissue and immune cells. Acta Biomater. 2014; 10(12):5202–12. [PubMed: 25153780]

80. Tesler AB, Kim P, Kolle S, Howell C, Ahanotu O, Aizenberg J. Extremely durable biofouling-resistant metallic surfaces based on electrodeposited nanoporous tungstite films on steel. Nat Commun. 2015; 6:8649. [PubMed: 26482559]

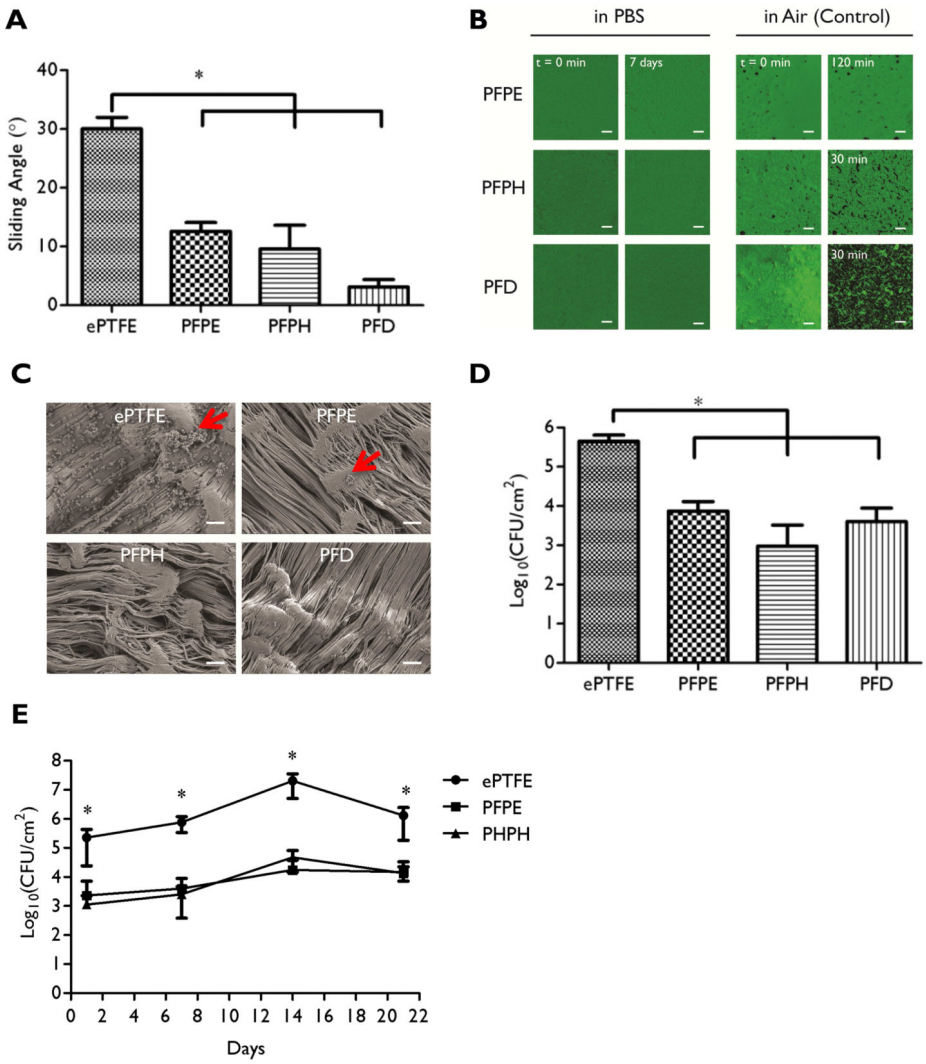

Figure 1. In vitro characterization of ePTFE-SLIPS and anti-bacterial adhesion behavior

(**A**) Slippery function of SLIPS was measured by tilting angle assay. (**B**) Reflection confocal microscopy images of lubricant-infused surfaces submerged over varying intervals in PBS or air. (**C**) SEM images of ePTFE or ePTFE-SLIPS after two days in culture with *S. aureus* (Scale bar: 10 μm). Red arrow: bacteria. (**D**) Colony-forming units (CFU) of ePTFE or ePTFE-SLIPS after exposure to *S. aureus* for two days. (**E**) CFU of ePTFE or ePTFE-SLIPS incubated in 50% rat serum for varying intervals and subsequently exposed to *S. aureus* for 48h. Error bars represent mean ± s.d. from at least 3 replicates, $*p < 0.05$, ePTFE vs PFPE, PFPH and PFD.

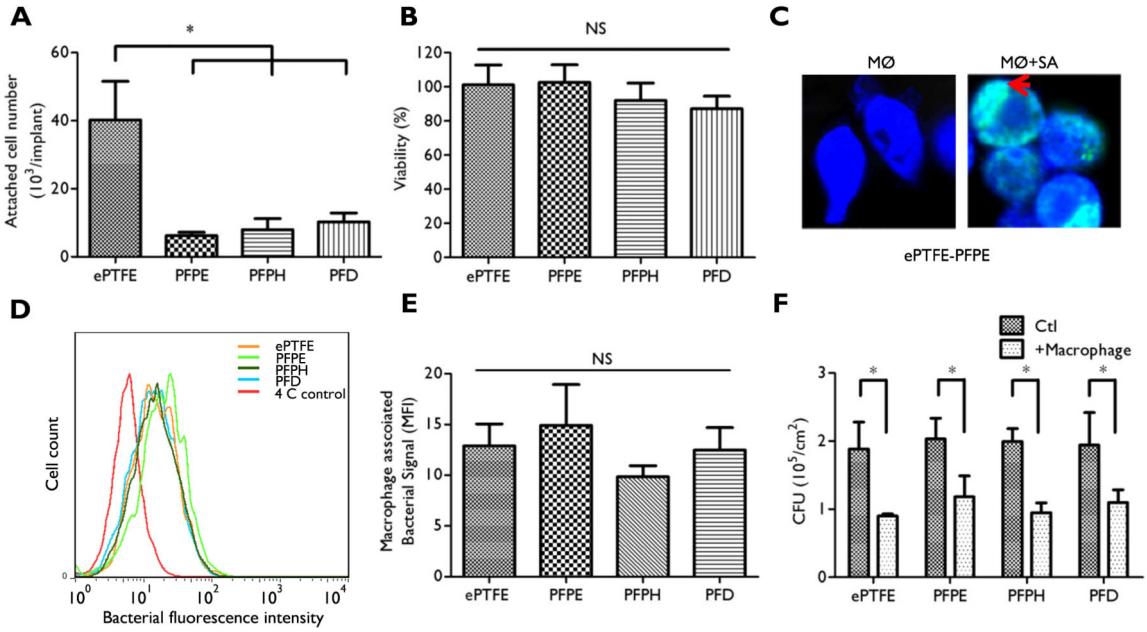

Figure 2. Macrophage behavior on ePTFE-SLIPS substrates

(**A**) Attachment of macrophages was measured by crystal violet (CV) staining after a 1 h incubation. (**B**) Macrophage viability was measured after a 24 h culture period by Alamar blue reduction. (**C**) Macrophage phagocytosis was visualized by confocal microscopy. CellTrace Violet-labeled macrophages (blue fluorescence) were exposed to Syto-9-labeled *S. aureus* (green fluorescence) for 30 min. MØ: macrophages; SA: *S. aureus*. Red arrow highlights engulfed bacteria. (**D**) Flow cytometry of bacterial phagocytosis by macrophages after a 1 h incubation period at 37°C or 4°C. (**E**) Phagocytosis was calculated by subtracting macrophage-associated fluorescence intensity at 4°C from that measured at 37°C. (**F**) The effect of SLIPS on bactericidal potential of macrophages. Macrophages were incubated with *S. aureus* for 2 h and viability was examined by a colony forming unit assay. Error bars represent mean ± s.d. from at least 3 replicates (*$p < 0.05$).

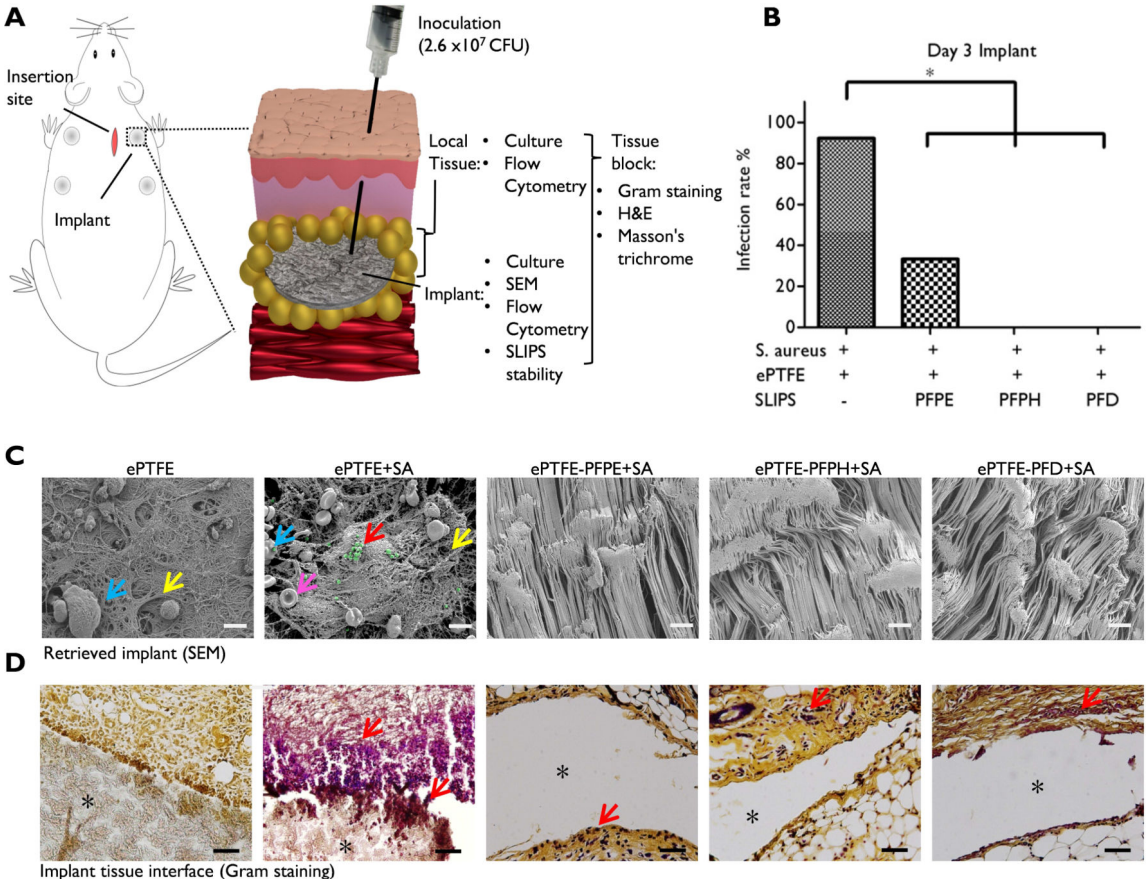

Figure. 3. Bacterial resistance of ePTFE-SLIPS in vivo

(**A**) Schematic of in vivo model. Circular implants (d = 6 mm) were surgically placed in the subcutaneous tissue on the dorsal side of rat. *S. aureus* (2.6×10^7 CFU, 50 μL) was injected 24 h later into the implant site. Three days after bacterial challenge, both the implant and local tissue were harvested. (**B**) Infection rate three days after inoculation. Implants were removed, minced, and sonicated in Luria-Bertani broth and cultured for 20 h at 37°C. Implants were considered infected if broth was turbid (as measured by OD600) and *S. aureus* was present on an agar plate of the culture. Infection rate (%) was calculated by dividing the number of infected implants by the total number of implants (*$p < 0.05$). (**C**) SEM images of retrieved implants three days after bacterial inoculation (Blue arrow: leukocytes; Yellow arrow: matrix; Red arrow: bacteria highlighted in green; Pink arrow: red blood cell; Scale bar: 10 μm). (**D**) Gram stain of implant-tissue interface (*S. aureus* dark purple, Red arrow: bacteria, *implant pocket, Scale bar: 100 μm).

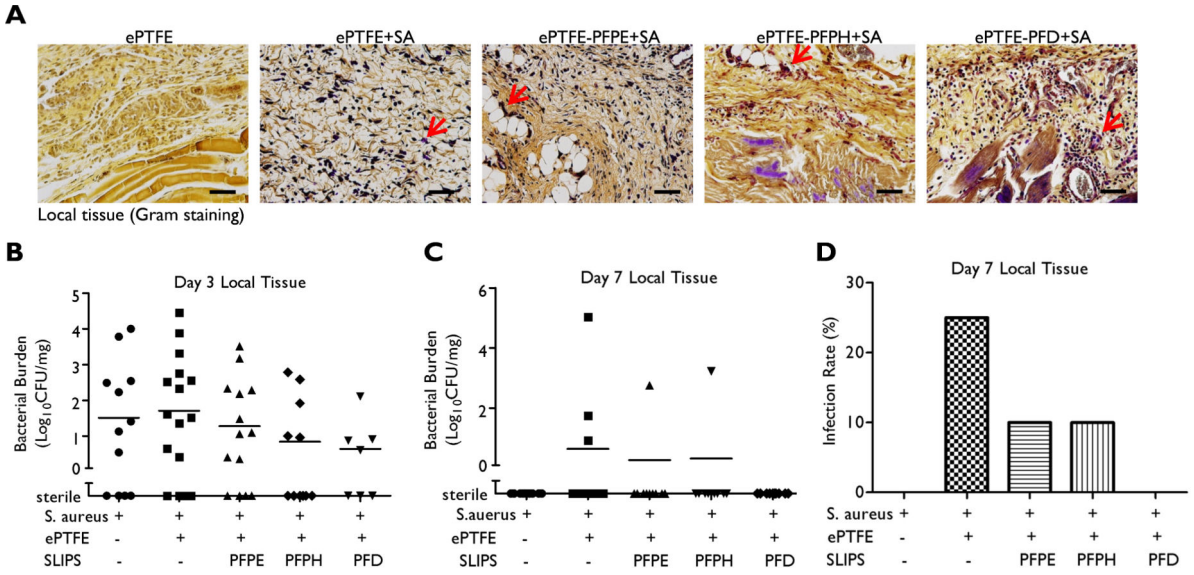

Figure. 4. Bacterial burden in peri-implant tissue

(**A**) Gram stain of peri-implant tissue (*S. aureus* dark purple, Red arrow: bacteria, Scale bar: 100 μm). (**B**) Bacterial CFU in local tissue three days and 7 days (**C**) after inoculation. Local tissue was collected, digested, diluted and plated on agar plate to count CFU, which was normalized by tissue weight. Results are presented from individual implants. (**D**) Infection rate was calculated at day 7 by dividing the number of infected tissue samples by total sample number.

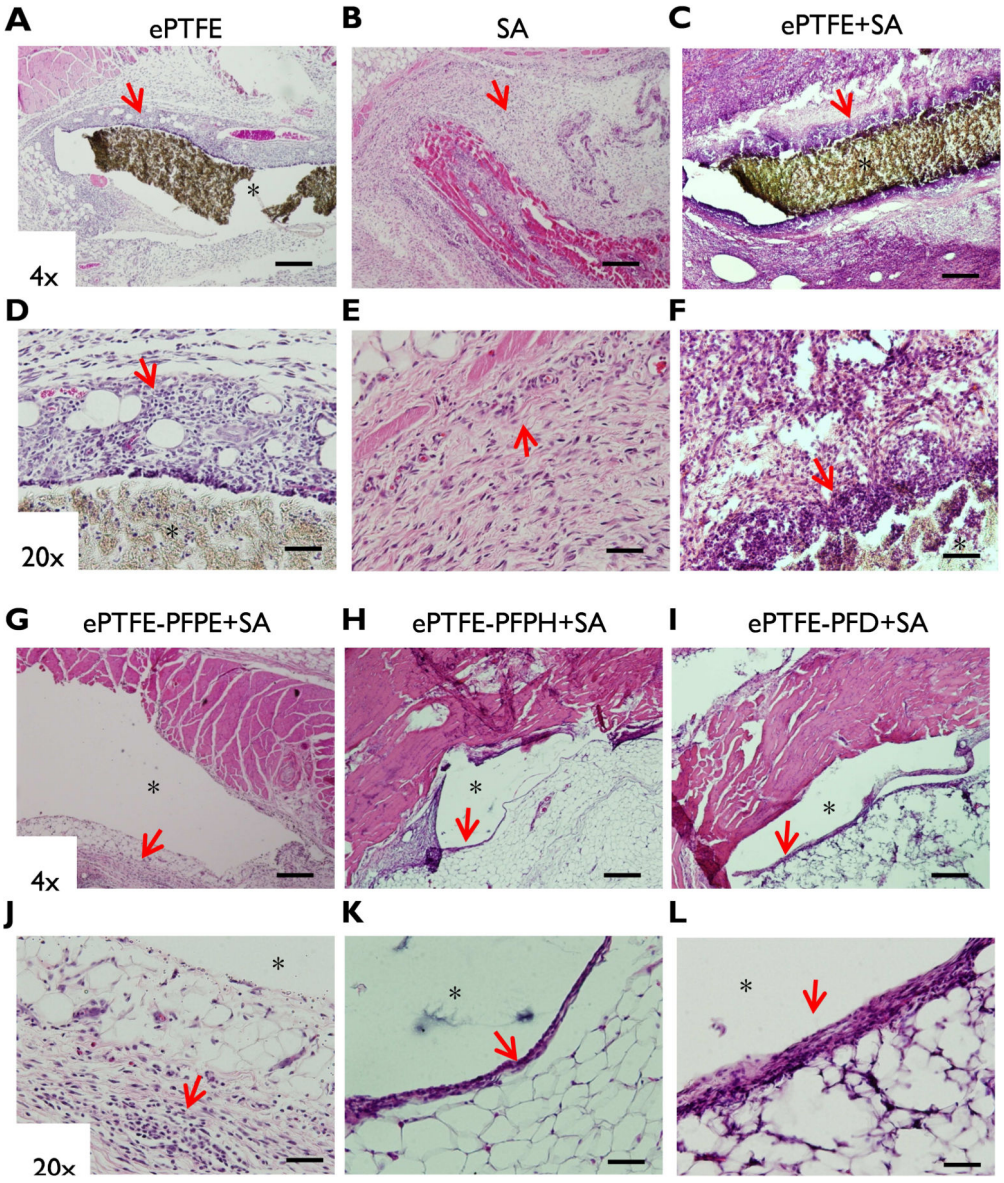

Figure 5. Histological staining of implants and peri-implant tissue

Three days after inoculation, whole tissue blocks were harvested for hematoxylin and eosin staining. (**A,D**) ePTFE alone. (**B,E**) *S.aureus* (SA) alone. (**C,F**) ePTFE+SA. (**G,J**) ePTFE +PFPE+SA. (**H,K**) ePTFE+PFPH+SA. (**I,L**) ePTFE+PFD+SA. (**A-C, G-I**) Magnification 4x. Scale bar: 1 mm. (**D-F, J-L**) Magnification 20x. Scale bar: 100 μm (*implant pocket). Red arrows highlight immune cell infiltration.

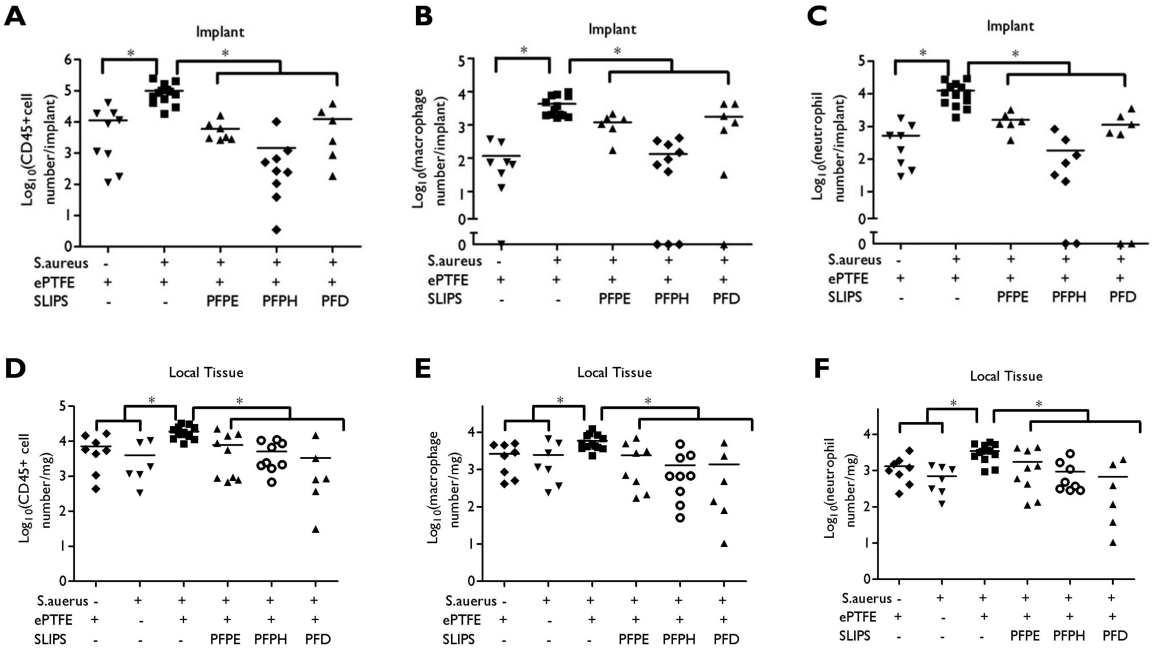

Figure 6. Flow cytometric analysis of inflammatory response within the vicinity of the implant and the peri-implant tissue

Three days after bacterial challenge, implants and surrounding tissue were harvested and digested with collagenase. Flow cytometry was performed with anti-CD45 (**A, D**), anti-neutrophil (**B, E**) and anti-macrophage antibodies (**C, F**). Results are presented from individual implants combined from at least two independent experiments (*$p < 0.05$).

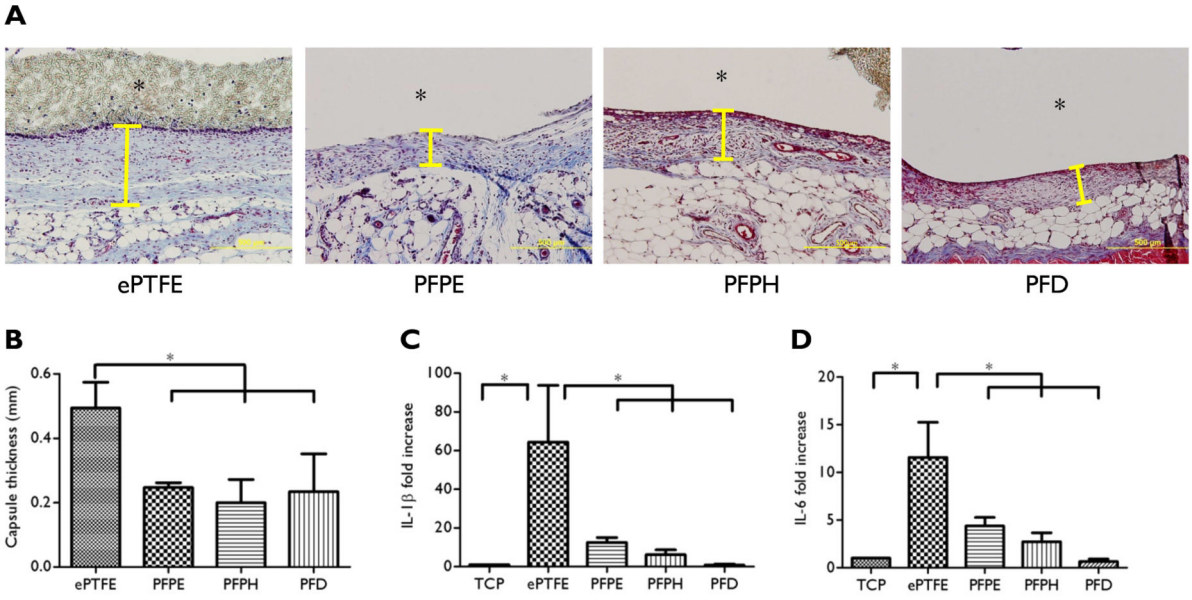

Figure 7. Host response to SLIPS at day 7

ePTFE or ePTFE-SLIPS implants (d = 6 mm) were harvested at 7 days. (**A**) Masson's trichrome staining demonstrated a substantially thinner capsule surrounding the ePTFE-SLIPS implant (Yellow line indicates capsule, *implant pocket, Scale bar: 500 μm). (**B**) Quantification of capsule thickness. (**C, D**) Effect of SLIPS on macrophage cytokine expression. Macrophages were cultured on tissue culture plastic (TCP), ePTFE or SLIPS-treated ePTFE for 18 hours and IL-1β and IL-6 measured by q-PCR. Error bars represent mean ± s.d. from at least 3 replicates, *$p < 0.05$.